RESEARCH ARTICLE

WILEY

Rhoptry neck protein 2 expressed in *Plasmodium* sporozoites plays a crucial role during invasion of mosquito salivary glands

Tomoko Ishino[1]* | Eri Murata[1,2]* | Naohito Tokunaga[1] | Minami Baba[1] |
Mayumi Tachibana[1] | Amporn Thongkukiatkul[3] | Takafumi Tsuboi[2] | Motomi Torii[1]

[1]Division of Molecular Parasitology, Proteo-Science Center, Ehime University, Toon, Japan

[2]Division of Malaria Research, Proteo-Science Center, Ehime University, Matsuyama, Japan

[3]Department of Biology, Faculty of Science, Burapha University, Chonburi, Thailand

Correspondence
Tomoko Ishino, Division of Molecular Parasitology, Proteo-Science Center, Ehime University, Toon, Ehime 791-0295, Japan.
Email: tishino@m.ehime-u.ac.jp

Present Address
Naohito Tokunaga, Division of Analytical Bio-Medicine, the Advanced Research Support Center (ADRES), Ehime University, Toon, Ehime 791-0295, Japan.

Abstract

Malaria parasite transmission to humans is initiated by the inoculation of *Plasmodium* sporozoites into the skin by mosquitoes. Sporozoites develop within mosquito midgut oocysts, first invade the salivary glands of mosquitoes, and finally infect hepatocytes in mammals. The apical structure of sporozoites is conserved with the infective forms of other apicomplexan parasites that have secretory organelles, such as rhoptries and micronemes. Because some rhoptry proteins are crucial for *Plasmodium* merozoite infection of erythrocytes, we examined the roles of rhoptry proteins in sporozoites. Here, we demonstrate that rhoptry neck protein 2 (RON2) is also localized to rhoptries in sporozoites. To elucidate RON2 function in sporozoites, we applied a promoter swapping strategy to restrict *ron2* transcription to the intraerythrocytic stage in the rodent malaria parasite, *Plasmodium berghei*. *Ron2* knockdown sporozoites were severely impaired in their ability to invade salivary glands, via decreasing the attachment capacity to the substrate. This is the first rhoptry protein demonstrated to be involved in salivary gland invasion. In addition, *ron2* knockdown sporozoites showed less infectivity to hepatocytes, possibly due to decreased attachment/gliding ability, indicating that parts of the parasite invasion machinery are conserved, but their contribution might differ among infective forms. Our sporozoite stage-specific knockdown system will help to facilitate understanding the comprehensive molecular mechanisms of parasite invasion of target cells.

KEYWORDS

conditional knockdown, malaria, rhoptry, sporozoite

1 | INTRODUCTION

Plasmodium parasites are the causative agents of malaria, a devastating infectious disease transmitted via mosquitoes. Approximately half a million people worldwide die from malaria each year (WHO, 2017).

Plasmodium parasites are eukaryotic unicellular organisms that transform into two different infective forms, merozoites and sporozoites, to complete a complex life cycle between mammals and mosquitoes. Sporozoites are formed in oocysts at the basal lamina of midguts in mosquitoes and upon release invade the salivary glands of mosquitoes, from which they are inoculated into mammalian skin during a blood meal (Ghosh & Jacobs-Lorena, 2009). Transmission is completed

*These authors contributed equally to this work.

by their migration to the liver and infection of hepatocytes. Salivary gland invasion is essential for malaria transmission and requires sporozoite attachment to the basal lamina of salivary glands, invasion of gland cells, followed by migration into the secretory cavity (reviewed in Mueller, Kohlhepp, Hammerschmidt, & Michel, 2010; Smith & Jacobs-Lorena, 2010).

Gene manipulation strategies have revealed several sporozoites proteins essential for invasion of salivary glands. Many of them, such as thrombospondin-related adhesive protein (TRAP; Ejigiri et al., 2012; Sultan et al., 1997), TRAP-related protein/upregulated in oocyst sporozoite 3 (TREP/S6/UOS3; Combe et al., 2009; Mikolajczak et al., 2008; Steinbuechel & Matuschewski, 2009), sporozoite invasion association protein-1 (SIAP-1; Engelmann, Silvie, & Matuschewski, 2009), and inhibitor of cysteine proteases (ICP; Boysen & Matuschewski, 2013), are involved in sporozoite motility, which is crucial for salivary gland invasion. TRAP is a type-I transmembrane protein, containing a thrombospondin type-I repeat domain and a von Willebrand factor-like A domain in its extracellular region, which is released to the cellular membrane and translocated to the posterior pole to move sporozoites forward (reviewed in Morahan, Wang, & Coppel, 2008). In contrast, membrane-associated erythrocyte binding-like protein (MAEBL), a chimeric secretory protein with an AMA1-like N-terminus and a C-terminus similar to erythrocyte-binding antigen 175, is dispensable for sporozoite motility in vitro, but crucial for salivary gland invasion, possibly via mediating interaction with basal lamina and/or gland cells (Kariu, Yuda, Yano, & Chinzei, 2002; Saenz, Balu, Smith, Mendonca, & Adams, 2008). Most of the proteins listed above are also involved in sporozoite transmission to mammalian hosts, indicating that sporozoite motility and attachment ability are important for invasion of different target cells—specifically, salivary glands in mosquitoes and hepatocytes in mammals.

Sporozoites, as well as other infective forms of the apicomplexan protozoa that can develop and proliferate within a parasitophorous vacuole formed in host cells, contain secretory organelles at the apical end, such as micronemes and rhoptries. Micronemal proteins such as TRAP, TREP/S6/UOS3, and MAEBL have been elucidated by reverse genetics to be involved in parasite motility and/or attachment ability, mainly in *Plasmodium* sporozoites, as described above. In contrast, secretory proteins localized to the neck region of rhoptries have been predominantly characterized in *Plasmodium* merozoites and *Toxoplasma* tachyzoites, where they have been shown to be critical for target cell invasion. During parasite invasion, a tight junction forms between the parasite tip and the host cell, facilitating parasite entry (Aikawa, Miller, Johnson, & Rabbege, 1978). A number of rhoptry neck proteins (RONs), including RON2, RON4, and RON5, are secreted and inserted into the target cellular membrane as a complex (Besteiro, Michelin, Poncet, Dubremetz, & Lebrun, 2009; Lebrun et al., 2005) and interact with apical membrane antigen 1 (AMA1), which is released from micronemes to the parasite plasma membrane (Cao et al., 2009; Tonkin et al., 2011; Vulliez-Le Normand et al., 2012). An interaction between RON2 and AMA1 has been shown, using inhibitory peptides or antibodies, and appears to be crucial for *Plasmodium* merozoite (Richard et al., 2010; Srinivasan et al., 2011; Tonkin et al., 2011) and *Toxoplasma* tachyzoite invasion (Lamarque et al., 2011; Tyler & Boothroyd, 2011).

The rhoptry neck proteins, RON2, RON4, and RON5, are also expressed at the apical region of sporozoites (Giovannini et al., 2011; Lindner et al., 2013; Mutungi, Yahata, Sakaguchi, & Kaneko, 2014; Tufet-Bayona et al., 2009), suggesting that rhoptry proteins also mediate sporozoite invasion of target cells, such as mosquito salivary glands and mammalian hepatocytes. It has been demonstrated that RON4 is secreted prior to invasion of hepatocytes (Risco-Castillo et al., 2014) and that it has crucial roles for infection of hepatocytes (Giovannini et al., 2011). Interaction between RON2 and AMA1 also may take place in sporozoites, as suggested by the result that inoculation of R1 peptide, which inhibits interaction between RON2 and AMA1 in *Plasmodium falciparum* merozoites, decreases both sporozoite cell traversal and invasion ability during sporozoite invasion of hepatocytes (Yang et al., 2017). Therefore, the aim of this study was to elucidate the function of sporozoite RON2 during salivary gland and hepatocyte invasion.

Reverse genetics approaches are powerful tools to elucidate protein roles; however, parasite genes that are essential for proliferation in the intraerythrocytic stage are typically intractable to DNA integration because homologous recombination occurs during the blood stage parasite development and, therefore, knockout parasites cannot be isolated. To overcome this problem, conditional gene silencing/disruption systems have been developed (Combe et al., 2009; Dvorin et al., 2010; Siden-Kiamos et al., 2011; Yap et al., 2014). Here, we modified the promoter swapping strategy for functional analysis of rhoptry proteins in sporozoites, specifically *ron2*, using the rodent malaria parasite strain, *Plasmodium berghei* ANKA (*Pb*ANKA), as an experimental model. By replacing the original *ron2* promoter with the *merozoite surface protein 1* (*msp1*) or *msp9* promoter, which are exclusively active at the intraerythrocytic schizont stage but inactive at the sporozoite stage, we successfully reduced RON2 expression to an undetectable level in sporozoites. We analysed the role of RON2 during sporozoite maturation and invasion of mosquito salivary glands and mammalian hepatocytes. The results demonstrate that sporozoite RON2 is required for salivary gland invasion, with a lesser contribution to hepatocyte invasion. This is the first report that a rhoptry protein plays a crucial role during sporozoite invasion of salivary glands. Our sporozoite stage-specific gene silencing system will facilitate the comprehensive understanding of rhoptry proteins, essential for invasion during the intraerythrocytic cycle, during sporozoite invasion of target cells in mosquitoes and in mammals.

2 | RESULTS

2.1 | RON2 expression profile in mosquito stage parasites

RON2, a key component of the AMA1-RONs complex formed at the moving junction between merozoites and erythrocytes, is expressed at the apical region of oocyst-derived sporozoites (Tufet-Bayona et al., 2009). To determine the RON2 expression profile during sporozoite maturation, Western blotting and real-time reverse transcription PCR (RT-PCR) analyses were performed using *Pb*ANKA strain parasites expressing green fluorescent protein (GFP) through the life cycle,

designated herein as GFP parasites (Franke-Fayard et al., 2004). A specific antibody against *P. berghei* RON2 (*Pb*RON2) was obtained from a rabbit immunised with a recombinant N-terminal region of *Pb*RON2 (RON2-N; amino acids 22–91) synthesized using a wheat germ cell-free protein production system (Arumugam et al., 2014; Tsuboi, Takeo, Arumugam, Otsuki, & Torii, 2010). To confirm the specificity of anti-RON2-N antibodies, Western blotting was performed using schizont-enriched transgenic parasites expressing RON2 fused with c-Myc at the C-terminus (RON2-c-Myc; see Figure S1). Anti-RON2-N antibodies detected the protein as a major band at above 250 kDa, as indicated by an open arrowhead, which is also recognised by anti-c-Myc antibodies, demonstrating that anti-RON2-N antibodies specifically recognise native *Pb*RON2 by Western blotting (Figure S1b). This size corresponds to its calculated molecular weight (236 kDa) and is like that of *P. falciparum* RON2 (Cao et al., 2009). Sporozoites form and mature in oocysts at the basal lamina of midguts, which are then released into the haemolymph and invade salivary glands in mosquito bodies. GFP sporozoites were collected from midgut oocysts,

haemolymph, and salivary glands of parasite-infected *Anopheles stephensi* (An. stephensi) mosquitoes to compare RON2 protein levels during sporozoite maturation—for comparison with schizont-enriched antigens prepared and used as a control. Within sporozoite lysates, RON2 protein was detected at a similar level and molecular weight as that in schizonts (Figure 1a), confirming that RON2 is expressed in sporozoites from the early developmental phase in oocysts until after invasion of salivary glands.

The relative amount of *ron2* mRNA was examined by real-time RT-PCR analysis using RNA extracted from sporozoites collected from midguts, haemolymph, and salivary glands of infected mosquitoes (Figure 1b). *Ron2* transcripts occur predominantly in developing oocyst stage sporozoites, although RON2 protein levels remain stable even after invasion of the salivary glands.

To refine RON2 localization in merozoites and sporozoites, immunotransmission electron microscopy (IEM) analysis was performed using RON2-c-Myc parasites. In mature merozoites, RON2 is clearly localized to the rhoptry neck region (Figure 1c, left) as reported in

FIGURE 1 RON2 expression profile in sporozoites. (a) Western blotting analysis of RON2 in sporozoites and schizonts. (Upper panel) 100,000 sporozoites collected from different body parts (MG: midgut; HL: haemolymph; SG: salivary gland) and 10,000 schizonts were separated by SDS-PAGE and transferred to PVDF membrane and then incubated with anti-RON2-N antisera. The sizes of the molecular weight markers are indicated on the left. RON2 was detected in all samples at approximately the predicted size (236 kDa) as indicated by the unfilled arrowhead. (Lower panel) Parasite antigen amount was confirmed with anti-HSP70 antisera (PbHSP70), indicated by the filled arrowhead. (b) *Ron2* transcription was measured by real-time RT-PCR using sporozoites collected from mosquito midguts, haemolymph, and salivary glands on days 17 to 21 post feeding. Relative *ron2* mRNA expression levels compared with midgut sporozoites are shown. Transcript levels were normalised to *ef1α* expression in the samples. Error bars: standard deviations among three samples. The *ron2* mRNA amount in oocyst-derived sporozoites is significantly higher than that in sporozoites collected from haemolymph or salivary glands (calculated by the one-way ANOVA with Tukey's multiple comparisons test (**$P < 0.01$). (c) Immunoelectron microscopy analyses of RON2-c-Myc fusion transgenic parasites. A merozoite (left panel) and sporozoites collected from midguts or salivary glands (middle and right panels) were fixed, and immunoelectron microscopy was performed using an anti-c-Myc antibody. RON2 is localized to rhoptries in both merozoite and sporozoite. Bars: 500 nm; R: rhoptry; M: microneme; D: dense granule; N: nucleus
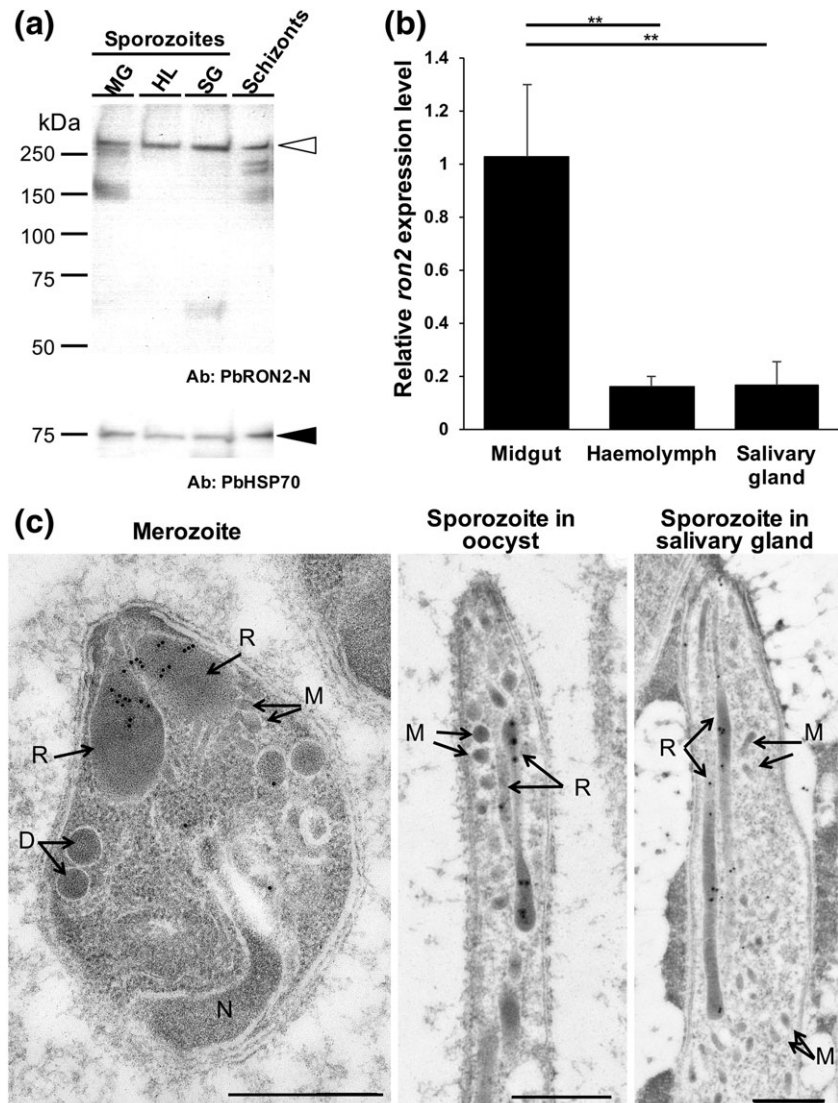
P. falciparum (Cao et al., 2009). In both oocyst and salivary gland sporozoites (Figure 1c, middle and right), RON2 is localized to the rhoptries; however, it is distributed throughout the rhoptry body rather than restricted to the neck region. This suggests that the rhoptry structure and/or protein secretion mechanisms differ in merozoites and sporozoites. Taken together, these results indicate that *ron2* transcription and translation occur mainly during sporogony in oocysts, and thereafter, the produced RON2 is retained in rhoptries until its secretion.

2.2 | Construction of the sporozoite stage-specific *ron2* knockdown parasites

Previous attempts to disrupt RON2, or to fuse a GFP-tag at its C-terminus, have failed (Tufet-Bayona et al., 2009); presumably because RON2 and its structure are essential for merozoite invasion of erythrocytes (Lamarque et al., 2011; Richard et al., 2010; Srinivasan et al., 2011; Tonkin et al., 2011; Tyler & Boothroyd, 2011). To examine RON2 function in sporozoites, we sought to develop a sporozoite stage-specific knockdown system—specifically, a promoter swapping method to restrict *ron2* transcription to the intraerythrocytic stage. To mimic the native *ron2* transcription pattern during the intraerythrocytic stage, the ideal candidate promoter to swap should be most active at the schizont stage but repressed in the sporozoite stage. Using in silico screening with a *P. falciparum* microarray and proteome data from PlasmoDB (Aurrecoechea et al., 2009) and RT-PCR analysis using *P. berghei* sporozoites and schizonts, we selected two candidate genes that matched these criteria. To confirm their transcription in oocyst-derived sporozoites and schizonts, real-time RT-PCR was performed. The relative transcription levels of *msp1* and *msp9* were approximately ninefold and 30-fold lower than *ron2* in oocyst-derived sporozoites; however, the transcription level of *rap1*, encoding a known rhoptry protein, was like that of *ron2* (Figure 2a). At the schizont stage, *rap1*, *msp1*, and *msp9* transcription levels were equal to or higher than that of *ron2* (Figure 2b), suggesting that swapping the *ron2* promoter with one of these promoters would retain RON2 function during merozoite invasion of erythrocytes. Therefore, a 1,051 bp segment of the *msp1*- and a 1,252 bp segment of the *msp9*–5′ untranslated region (UTR) were

selected as putative schizont-specific promoters to replace the *ron2* promoter. In addition, a 1,065 bp segment of the *rap1* putative promoter was used to generate control transgenic parasites, which would not affect RON2 expression in either sporozoites or merozoites (see Figures 3a and S2). The cloned transgenic parasites were named according to the promoter inserted before the RON2 coding region, that is, P_{rap1}-RON2 (control), P_{msp1}-RON2, and P_{msp9}-RON2. Correct DNA integration at the *ron2* locus and replacement of its native promoter region was confirmed by genotyping PCR using genomic DNA extracted from cloned transgenic parasites (Figure S3).

RON2 protein expression in schizonts was not affected by promoter swapping to either the *rap1* or *msp9* promoters (Figure S4a). Consequently, P_{msp9}-RON2 parasites could proliferate normally in the blood stage in vivo (Figure S4b). Next, to collect sporozoites, these transgenic parasite lines were transmitted from infected mice to *An. stephensi* mosquitoes by blood feeding. To examine the effects of *ron2* knockdown on the sporozoite development and expression of other rhoptry proteins and their trafficking to rhoptries, the subcellular localization of rhoptry-associated membrane antigen (RAMA; Topolska, Black, & Coppel, 2004) was observed by IEM. P_{msp9}-RON2 sporozoites developed and matured normally in oocysts (Figure S5a), and RAMA is localized to rhoptries, which are morphologically normal, in these sporozoites (Figure S5b), strongly indicating that RON2 is dispensable for rhoptry formation and RAMA trafficking to rhoptries.

Next, we confirmed the repression of *ron2* transcription and protein expression using oocyst-derived mutant sporozoites. As shown in Figure 3b, *ron2* mRNA levels in P_{msp1}-RON2 and P_{msp9}-RON2 sporozoites were approximately fivefold and 50-fold less, respectively, compared with GFP sporozoites. Western blotting using sporozoites purified from midguts of mosquitoes infected by GFP or transgenic parasites was performed to determine whether RON2 protein levels in promoter swapping sporozoites reflect the repression of *ron2* transcription. The band intensity corresponding to RON2 in 5.0×10^4 P_{msp1}-RON2 sporozoites (3.4×10^6) and that in 5.0×10^5 P_{msp9}-RON2 sporozoites (1.3×10^6) was like that in 1.0×10^4 GFP sporozoites (1.9×10^6) and P_{rap1}-RON2 (2.4×10^6; Figure 3c). These results, consistent with the relative RON2 band intensity compared with HSP70 (Figure S6), demonstrate that RON2 amount is decreased twofold to fivefold and approximately 50-
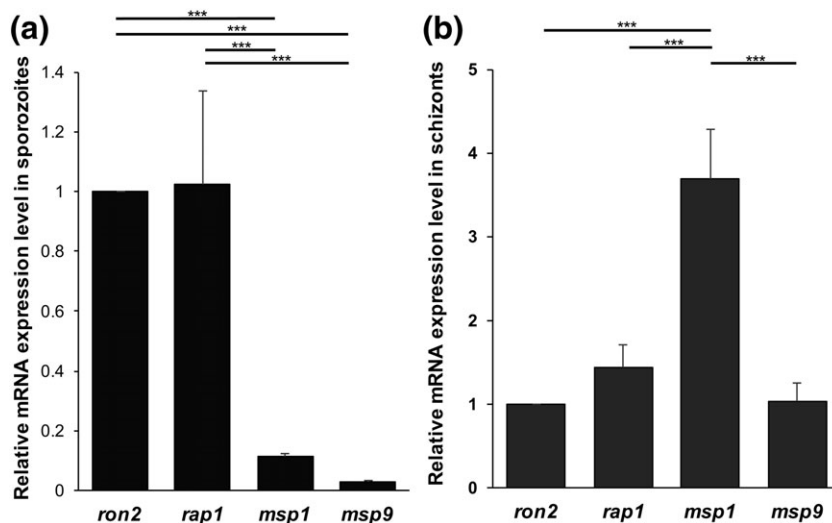
FIGURE 2 Promoter activity analyses using real-time RT-PCR. Comparison of *ron2*, *rap1*, *msp1*, and *msp9* mRNA expression level in midgut sporozoites (a) and in schizonts (b). Midguts were collected from GFP parasite-infected mosquitoes at day 18 post feeding, and schizonts were purified by density gradient centrifugation for RNA extraction. Bars indicate the relative transcription levels of each gene compared with *ron2* expression in midgut sporozoites (a) or in schizonts (b) with the standard deviations from three independent experiments. Statistical differences were calculated by the one-way ANOVA with Tukey's multiple comparisons test (***$P < 0.005$)
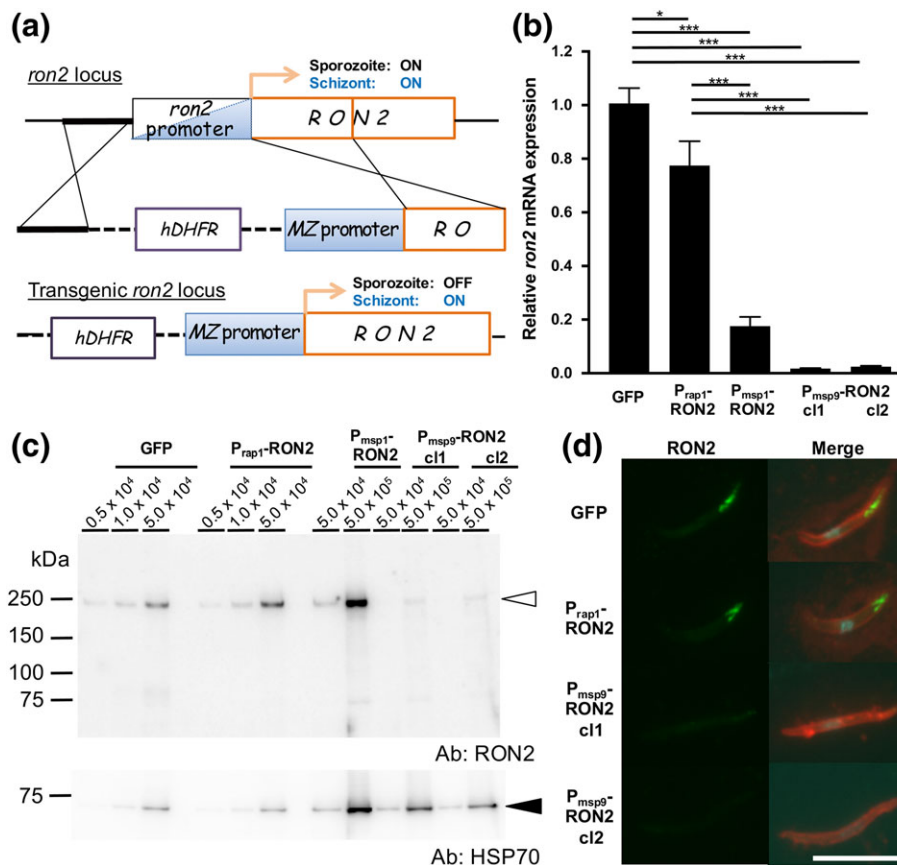
FIGURE 3 Construction of sporozoite stage specific *ron2* silencing transgenic parasite. (a) Schematic representation of genomic DNA modification by double cross-over homologous recombination. To restrict *ron2* expression to intraerythrocytic stage parasites, the predicted *ron2* promoter region (*ron2* promoter) was replaced by a promoter region that is active predominantly in schizonts (*MZ* promoter). For selection of transgenic parasites, the human DHFR expressing cassette (*hDHFR*) was inserted as a drug selection marker. The resulting genetically modified parasites should express RON2 only in schizonts, and not in sporozoites. (b) Measurement of *ron2* transcription in oocyst-derived sporozoites. RNA was extracted from parasite-infected midguts collected at days 17 or 18 post feeding and then subjected to real-time RT-PCR analysis. The relative values for *ron2* expression, normalised to *rama* expression, are shown as bars with standard deviations. Swapping the *ron2* promoter to the *msp1* or *msp9* promoter resulted in approximately fivefold or 50-fold reduction in *ron2* transcription compared with the control. Error bars: standard errors among five independent experiments. Statistical differences were calculated by the one-way ANOVA with Tukey's multiple comparisons test (***$P < 0.005$; *$P < 0.05$). (c) Comparison of RON2 protein amount in oocyst-derived sporozoites. Transgenic sporozoites were collected from midguts at days 21–26 post feeding, and the indicated number of sporozoites was loaded on the gel for Western blotting analysis using anti-RON2-N antisera. In GFP sporozoites, the RON2 signal, indicated by an unfilled arrowhead, was clearly detected with 5.0×10^4 sporozoites, whereas only faint or no signal could be detected in P_{msp1}-RON2 or P_{msp9}-RON2 sporozoites, respectively. The lower panel shows the antigen amount by HSP70 detection, indicated by a filled arrowhead. (d) RON2 localization in GFP, P_{rap1}-RON2, or P_{msp9}-RON2 haemolymph sporozoites. Sporozoites were collected from haemolymph at days 21 to 24 post feeding, fixed by acetone and then incubated with anti-RON2-N antibodies (green) and anti-CSP monoclonal antibodies (red). Nuclei were stained with DAPI (cyan). Parasite cytosolic GFP signal was destroyed by the acetone treatment. The typical apical-end signal of RON2 detected in GFP and P_{rap1}-RON2 sporozoites was absent in P_{msp9}-RON2 sporozoites, confirming that RON2 expression in sporozoites is significantly repressed by promoter exchange. Bar: 10 μm. More images for each parasite line were demonstrated in Figure S9

fold by replacing its promoter to *msp1* or *msp9* promoters, respectively. In addition to assays of RON2 levels, two representative micronemal proteins TRAP and AMA1 were detected by Western blotting using oocyst-derived sporozoites. As shown in Figure S7, the levels of TRAP and AMA1 were not correlated to the amount of RON2 in sporozoites, suggesting that *ron2* promoter swapping exclusively influenced RON2 expression, and not micronemal proteins.

After maturation in oocysts, sporozoites egress into the mosquito haemolymph and then invade salivary glands. Therefore, we next examined whether *ron2* knockdown by promoter swapping continues in salivary gland resident sporozoites. As shown in Figure S8, the RON2 amount in P_{msp1}-RON2 or P_{msp9}-RON2 sporozoites remains decreased

or undetectable level in sporozoites released into the haemolymph and residing in salivary glands. It was confirmed by immunofluorescence analysis (IFA) that the typical RON2 signals at the apical end, observed in GFP and P_{rap1}-RON2 haemolymph sporozoites, were almost undetectable in each P_{msp9}-RON2 sporozoite (Figures 3d and S9).

2.3 | RON2 plays an important role in sporozoite invasion of salivary glands

To elucidate the role of RON2 in the sporozoite stages, from development in oocysts to the invasion of salivary glands, the following

experiments were conducted using transgenic parasites. Mosquito groups were used that showed >80% oocyst prevalence, determined by oocyst detection at day 10 post feeding. The numbers of sporozoites collected from midguts, haemolymph, or salivary glands were determined from GFP, control (P_{rap1}-RON2), P_{msp1}-RON2, and P_{msp9}-RON2 parasite-infected mosquitoes. The average numbers of midgut and haemolymph sporozoites were not significantly different among all lines, indicating that RON2 is dispensable for sporogony and sporozoite release into the haemolymph (Figure 4). These data are consistent with the observation that sporozoite budding and rhoptry formation occurred normally inside P_{msp9}-RON2 oocysts (Figure S5). In contrast, sporozoite numbers collected from salivary glands were approximately 20-fold lower in P_{msp1}-RON2 and P_{msp9}-RON2 parasite lines than in GFP or control parasites (Figure 4, right graph). This significant reduction in the number of salivary gland sporozoites demonstrates that sporozoite RON2 is crucial for salivary gland invasion.

Confocal laser scanning microscopy demonstrated that the numbers of P_{msp9}-RON2 sporozoites inside salivary glands were low, confirming that most RON2 repressed sporozoites failed to invade salivary glands (Figure 5). Although the total number of sporozoites in salivary gland lobes was greatly reduced by $ron2$ knockdown, the location of the invaded P_{msp9}-RON2 sporozoites in salivary glands was similar to that of GFP and P_{rap1}-RON2; that is, most sporozoites were found inside lobes and a few accumulated in the secretory cavity region. These data suggest that RON2 is involved in an initial step of sporozoite invasion of salivary glands—specifically, migration, recognition, or attachment to the salivary glands.

Sporozoite motility was shown to be critical for invasion of salivary glands by targeted gene disruption of TRAP (Ejigiri et al., 2012; Sultan et al., 1997), TREP/S6/UOS3 (Combe, Moreira, et al., 2009; Mikolajczak et al., 2008; Steinbuechel & Matuschewski, 2009), LIMP (Santos et al., 2017), ICP (Boysen & Matuschewski, 2013), actin capping protein (CP, Ganter, Schüler, & Matuschewski, 2009), and plasmepsin VIII (Mastan, Narwal, Dey, Kumar, & Mishra, 2017). Therefore, we examined the sporozoite motility of P_{msp9}-RON2 haemolymph sporozoites in vitro. Sporozoites, incubated with fatal calf serum (FCS), first attach to the glass slide followed by circular movement named gliding. The population of drifting sporozoites was increased in P_{msp9}-RON2 sporozoites approximately twofold than that in control, suggesting that attachment ability is decreased by $ron2$ knockdown (Figure 6). In accordance, the mean ratio of gliding sporozoites was 46 ± 9% in P_{rap1}-RON2 and 18 ± 7% and 21 ± 6% in P_{msp9}-RON2 cl1 and cl2. Taken together, the data suggests that RON2 is involved in sporozoite attachment to the substrate that initiates gliding. To further explore sporozoite interactions with substrates and gliding, sporozoites were embedded in Matrigel, composed of laminin and type IV collagen, to examine the motility when they are attached to the substrate. By classifying sporozoites moving patterns into three categories—non-motile, circular movement, and meandering, according to Volkmann et al. (2012)—no significant difference was observed between control and P_{msp9}-RON2 sporozoites (Figure S10a). In addition, the velocity of circular moving sporozoites is comparable between control and $ron2$ knockdown sporozoites (Figure S10b), suggesting that the gliding machinery based on actin–myosin motor system is not affected by $ron2$ knockdown.

2.4 | RON2 is required for sporozoite transmission to mammalian hosts

During blood meals, mosquitoes inject salivary gland resident sporozoites into the skin together with saliva. Therefore, we next examined whether RON2 is involved in parasite transmission to mammalian hosts by the natural route of the mosquito vector. C57BL/6 mice were fed by groups of mosquitoes infected by P_{rap1}-RON2, P_{msp1}-RON2, or P_{msp9}-RON2 parasites at days 21–22 post feeding. Parasite levels in the liver at 42 hr post inoculation were examined using real-time RT-PCR to measure the levels of parasite 18S ribosomal RNA (18S rRNA), normalised to mouse *glyceraldehyde-3-phosphate dehydrogenase* (*gapdh*) mRNA. As shown in Figure 7, the efficiency of parasite transmission to mice was significantly reduced about 50- to 100-fold by $ron2$ knockdown. To clarify whether this reduction in transmission
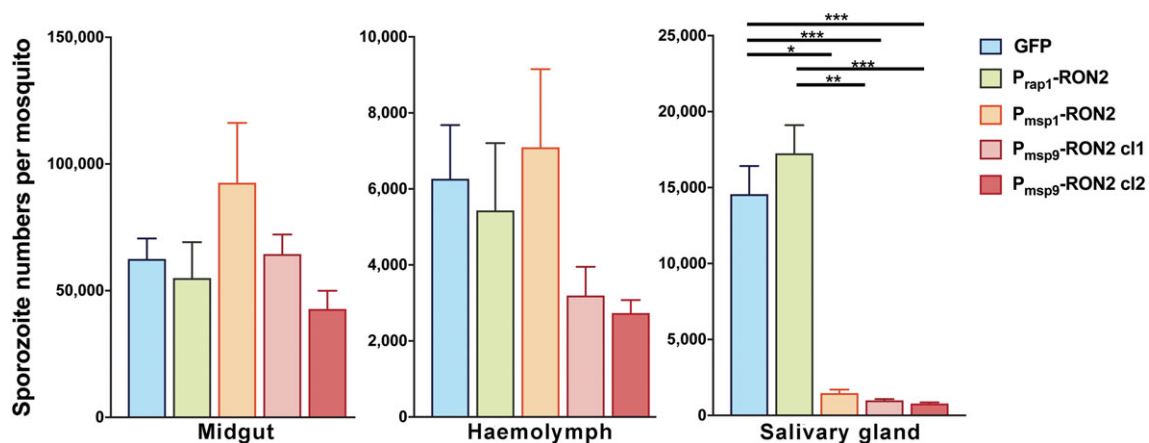
FIGURE 4 Sporozoite RON2 is involved in salivary gland invasion. The numbers of sporozoites collected from midguts, haemolymph, and salivary glands at days 21–24 post feeding were compared among transgenic parasite lines. Average numbers of sporozoites from each body part per mosquito from >20 mosquitoes are shown with error bars indicating the standard errors from at least five independent experiments. Sporozoite numbers collected from midguts and haemolymph are similar among all lines, whereas those from salivary glands were significantly reduced by RON2 repression, analysed by the Kruskal–Wallis test with a Dunn's post hoc test (*$P < 0.05$; **$P < 0.01$; ***$P < 0.005$)
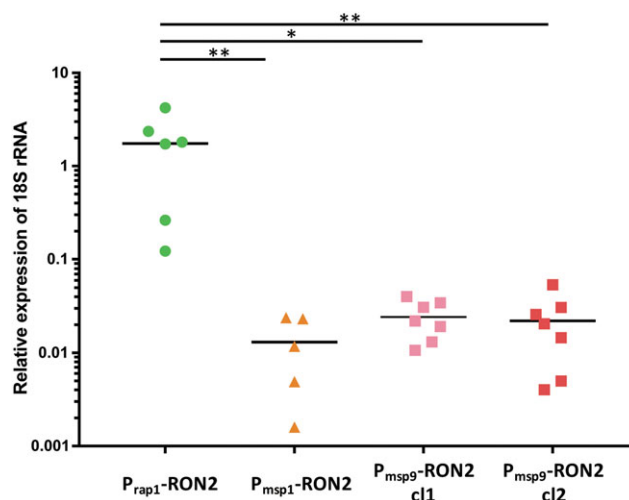
FIGURE 5 Detection of RON2-repressed sporozoites inside salivary glands. Salivary glands of GFP-, P_{rap1}-RON2-, or P_{msp9}-RON2-infected mosquitoes were dissected at day 22 post feeding and stained with FM4-64 (cellular membrane, red) and DAPI (nuclei, blue) and then observed by confocal laser microscopy. Sporozoites were detected by the GFP signal (green). GFP and P_{rap1}-RON2 sporozoites accumulate abundantly in salivary glands, especially in the secretory cavity. The number of P_{msp9}-RON2 sporozoites residing in salivary glands is limited; however, their distribution in salivary glands is similar to control sporozoites. Merged images for 5 μm thickness are shown. Bars, 50 μm
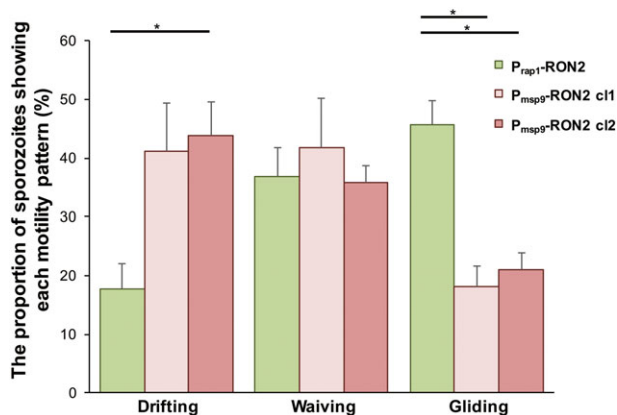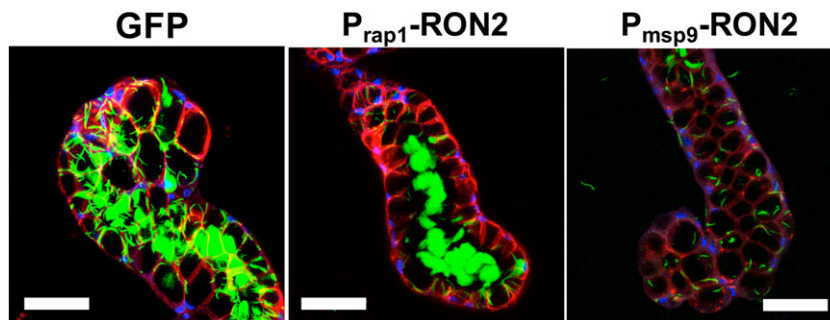
FIGURE 6 Comparison of sporozoite motility among transgenic parasite lines. Gliding ability of sporozoites collected from haemolymph at days 17–23 post feeding was examined in vitro. P_{rap1}-RON2, P_{msp9}-RON2 cl1, or cl2 sporozoites were incubated in 10% FCS containing RPMI 1640 medium in a glass bottom dish, then their movement was recorded every 2 s for about 5 min. Drifting, waving, and gliding sporozoite numbers were counted according to the criteria described in Hegge, Kudryashev, Smith, and Frischknecht (2009). Experiments were repeated four to five times with at least 75 sporozoites per parasite line. Bar graphs demonstrate the percentage of sporozoites showing each motility pattern with error bars indicating standard errors. The statistical difference in the percentage of gliding sporozoites between P_{rap1}-RON2 and P_{msp9}-RON2 were calculated by the Mann–Whitney U test (*$P < 0.05$)

FIGURE 7 Parasite transmission to mice via infected mosquito bites was greatly reduced by *ron2* knockdown. Groups of infected mosquitoes of indicated parasite lines at days 21–22 post feeding were fed on C57BL/6 mice, and the livers were harvested at 42 hr after biting. The graph shows the relative amounts of Pb18S rRNA with the mean values from five to seven experiments. The statistical differences in the relative expression of Pb18S rRNA among examined parasite lines were calculated by the Kruskal–Wallis test with a Dunn's post hoc test (*$P < 0.05$; **$P < 0.01$)

efficacy of *ron2* knockdown sporozoites is solely due to fewer numbers of sporozoites residing in salivary glands, further experiments on hepatocyte infection were performed as follows.

Once inoculated into the mammalian skin by mosquito bite, sporozoites migrate to the liver via the blood stream and efficiently infect hepatocytes. The report that RON4 is secreted and plays an important role during sporozoite invasion of hepatocytes (Giovannini et al., 2011; Risco-Castillo et al., 2014) raised the possibility that RON2 is also involved in sporozoite infection of hepatocytes. Sporozoites collected from salivary glands of mosquitoes infected with P_{rap1}-RON2 (control) or P_{msp9}-RON2 parasites were intravenously injected into C57BL/6 mice. The relative 18S rRNA level of P_{msp9}-RON2 parasites in the liver at 24 hr post inoculation was approximately 31% of that

control parasites (Figure 8a). This result indicates that RON2 has one or more roles during sporozoite infection of the liver, which includes the following steps: migration towards hepatocytes via blood stream, traversing the sinusoidal cell layer, invasion of hepatocytes with parasitophorous vacuole formation, and proliferation inside hepatocytes.

To examine the sporozoite cell traversal ability required for sporozoite migration in the skin and crossing the sinusoidal cell layer (Ishino, Yano, Chinzei, & Yuda, 2004; Amino et al., 2008), in vitro cell wounding assays were performed using the mouse fibroblast cell line, 3T3-Swiss. The cell traversal ability of P_{msp9}-RON2 sporozoites, indicated by the number of wounded cells, was reduced to about 50% of control parasites (Figure 8b). Next, to investigate if RON2 is involved in the invasion of hepatocytes and the subsequent maturation inside cells, an in vitro sporozoite infection assay was applied
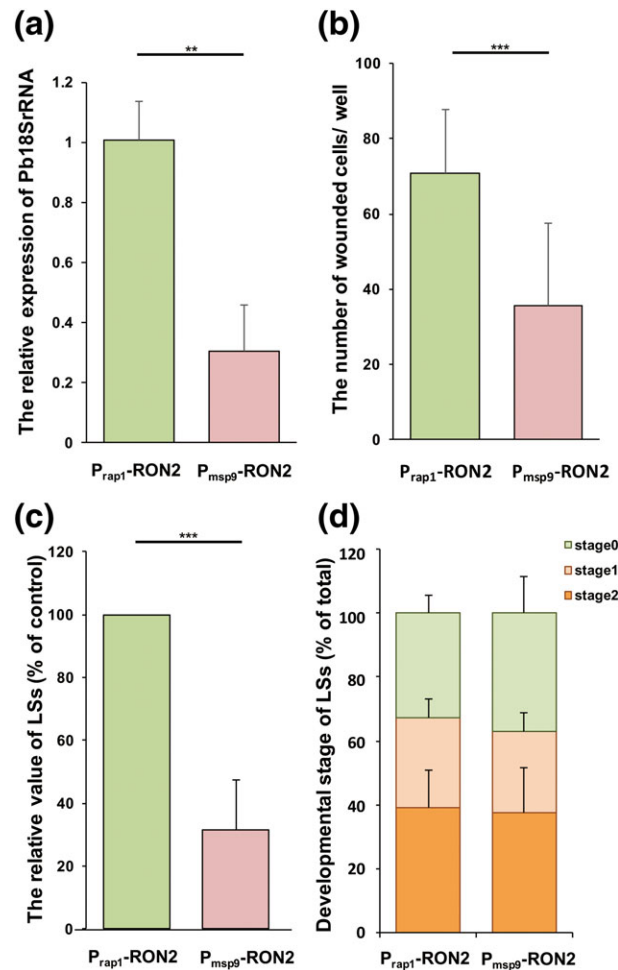
FIGURE 8 RON2 is also involved in hepatocyte invasion. (a) Infectivity of RON2 repressed sporozoites in mice. Equal numbers of P_{rap1}-RON2 or P_{msp9}-RON2 cl1 sporozoites (5 or 10 thousand) were inoculated into C57BL/6 mice 24 hr prior to the livers being collected to measure parasite 18S rRNA levels. The average values of relative parasite 18S rRNA levels, normalised to mouse *gapdh* mRNA level, of six mice from two independent experiments are shown with standard deviations as error bars. The statistical difference in the relative expression of Pb18S rRNA between P_{rap1}-RON2 and P_{msp9}-RON2 were calculated by the Mann–Whitney U test (**$P < 0.01$). (b) Cell traversal ability of sporozoites was examined by a cell wounding assay using fluorescence-conjugated dextran. Ten thousand haemolymph sporozoites collected from P_{rap1}-RON2 or P_{msp9}-RON2 cl1 infected mosquitoes were inoculated onto 3T3-Swiss cells, murine fibroblast-derived cultured cells, cultured in an eight-well chamber slide. Cells were incubated for 1 hr with 1 mg/ml of fluorescence-conjugated dextran (10,000 MW) in RPMI 1640 containing 10% FCS. Cells were washed with PBS and fixed with 10% formalin to detect cells damaged by sporozoites. Bars indicate the mean numbers of cells harbouring dextran per well with standard deviations from four independent experiments containing more than three wells. The numbers of damaged cells per well decreased significantly following *ron2* knockdown (calculated by the Mann–Whitney U test (***$P < 0.005$). (c and d) Infectivity of RON2 repressed sporozoites in hepatoma cells in vitro. Equal numbers of P_{rap1}-RON2 or P_{msp9}-RON2 cl1 sporozoites (4 to 10 thousand) were inoculated into HepG2 cells cultured in an eight-well chamber slide and then incubated for 2 days. (c) The mean of relative values of P_{msp9}-RON2 LSs, normalised to those of P_{rap1}-RON2, were shown in a graph with a standard deviation as an error bar. Experiments were repeated seven times with more than three wells for each parasite line. The statistical difference in the relative LS number between P_{rap1}-RON2 and P_{msp9}-RON2 were calculated by the Mann–Whitney U test (***$P < 0.005$). (d) LS developmental stage was categorised by maturation level, determined by LISP2 localization pattern (Itani et al., 2014). The percentage of each stage LS are shown with standard deviations as error bars. Stage 0, very young LS without LISP2 expression; stage 1, middle stage LS, where LISP2 remains inside the parasite; and stage 2, mature LS where LISP2 is transported to the host cell cytosol. Experiments were repeated five times with three wells for each parasite line

using the human hepatoma cell-line, HepG2. Two days after sporozoite inoculation into HepG2 cells, the number of liver stage (LS) parasites and their maturation levels were compared between control and P_{msp9}-RON2 parasites. LS parasite numbers and maturation were determined by IFA using anti-circumsporozoite protein (CSP) antibody (Mueller et al., 2005), together with an anti-liver stage specific protein 2 (LISP2) antibody, which serves as an LS maturation marker (Itani,

Torii, & Ishino, 2014). The total number of P_{msp9}-RON2 LS was decreased to approximately 32% of that of the control parasites (Figure 8c); however, the proportion of fully matured LS was similar to that of the control (Figure 8d). These results indicate that RON2 plays an important role during sporozoite invasion of hepatocytes, in addition to its more robust role during the invasion of salivary glands, but it is not important for subsequent intracellular LS development.

3 | DISCUSSION

3.1 | Sporozoite RON2 is important for parasite invasion of target cells

RON2 is well conserved among apicomplexan protozoa, such as *Plasmodium* spp., *Babesia*, *Theileria*, *Toxoplasma*, *Neospora*, and *Eimeria*. It has been demonstrated that RON2 and AMA1 interaction is a critical step for *Plasmodium* merozoite and *Toxoplasma* tachyzoite invasion of target cells (Lamarque et al., 2011; Richard et al., 2010). Here, we demonstrated that RON2 is also expressed and localized to rhoptries in *Plasmodium* sporozoites and is required for invasion of mosquito salivary gland cells and mammalian hepatocytes, which are necessary steps for malarial transmission.

Toxoplasma, *Neospora*, and *Eimeria* contain paralogous versions of *ron2* and *ama1*, which are specifically expressed in sporozoites, indicating that gene duplication events underpinned the evolution of differential gene regulation or protein function in tachyzoites versus sporozoites (Poukchanski et al., 2013). In contrast, *Plasmodium* species have a single *ron2* locus in the genome; therefore, it is reasonable that RON2 functions at both infectious stages, merozoites and sporozoites. It would be interesting to determine whether the AMA1-RON complex-dependent invasion mechanisms are also functioning during sporozoite invasion or whether RON2 has different counterparts in sporozoites.

3.2 | Sporozoite stage-specific *ron2* knockdown by promoter swapping

To optimise the promoter swapping system for elucidation of RON2 roles in sporozoites, two genes (*msp1*, *msp9*) were selected as candidate promoters to swap with *ron2* promoter based on the following two criteria: (1) an expression profile similar to that of *ron2* in the intraerythrocytic stages and (2) transcription is repressed in midgut sporozoites. Transcription timing and level can be affected by *cis*-elements in the promoter region and their interaction with transcriptional regulators such as ApiAP2s. Two candidate genes, as well as *ron2* and *rap1*, contain a "gtgca" motif in their promoter region, a target sequence of an ApiAP2 family protein (PF3D7_0604100) that regulates the expression of invasion related proteins in schizonts (Campbell, De Silva, Olszewski, Elemento, & Llinás, 2010; De Silva et al., 2008; Young et al., 2008). Moreover, a new gene category based on transcriptome analysis using 11 types of ApiAP2 knockout parasites (Modrzynska et al., 2017) also classified *msp1* and *msp9* in rhoptry protein-enriched clusters. This classification offers a logical basis for selecting suitable replacement promoters to elucidate other protein functions during the mosquito stages.

A conditional knockdown system utilising promoter swapping has advantages over a site-specific recombination method for analysing the functions of rhoptry proteins in sporozoites. For example, *ron2* transcription mainly occurs in oocyst-derived sporozoites (Figure 1b), and therefore, it could be difficult to activate a site-specific recombinase sufficiently prior to the onset of its transcription. The promoter swapping strategy enables continued repression of the target molecule from the start of the mosquito stage, and the repression remains even after sporozoite invasion of salivary glands (Figure S8). In addition, production of the target proteins could be suppressed to the same level in all mutant sporozoites obtained by promoter swapping, as demonstrated by RON2 expression in individual sporozoites (Figure 3d and S9). Our promoter swapping system using the *msp9* promoter can be applied not only for elucidating the functions of other rhoptry molecules but also those of the inner membrane protein family, the alveolins, which have a similar transcription pattern during the blood stages (Beck et al., 2013).

3.3 | Molecular mechanisms underlying sporozoite invasion of salivary glands

We revealed that RON2 in sporozoites is crucial for the invasion of salivary glands (Figure 4). The finding that P_{msp9}-RON2 sporozoites collected from salivary glands also showed a great reduction in RON2 levels (Figure S8) suggests that RON2 function might be compensated to some extent by other molecule(s), rather than invoking an explanation that a few sporozoites expressing RON2 at higher level could invade the salivary glands. Reduction in invasion ability of P_{msp1}-RON2 and P_{msp9}-RON2 was equivalent, although the RON2 amount was greater in P_{msp1}-RON2 than in P_{msp9}-RON2 sporozoites, indicating that a threshold of RON2 expression (at least more than 30% of GFP sporozoites) is required for invasion of salivary glands.

Previous electron microscopy analyses revealed that sporozoites first cross the basal membrane, invade the cytoplasm of gland cells, and then transverse to enter the secretory cavity (Pimenta, Touray, & Miller, 1994; Sterling, Aikawa, & Vanderberg, 1973). The confocal laser microscope image of salivary glands from P_{msp9}-RON2 infected mosquitoes discounted the possibility that *ron2* knockdown sporozoites remain attached to the basal lamina of salivary glands (Figure 5). Because sporozoites are passively transported through the mosquito haemocoel to salivary glands (Douglas, Amino, Sinnis, & Frischknecht, 2015), this suggests that RON2 is required for the recognition of, attachment to, or crossing of the basal lamina of salivary glands—in good agreement with the results demonstrating that RON2 is required for in vitro attachment/gliding ability. Following *ron2* knockdown, the ratio of gliding sporozoites was decreased as a result of an increase of drifting sporozoites (Figure 6). This agrees with the report that sporozoites need to attach to glass slides at both ends prior to starting circular migration (Münter et al., 2009; Hegge et al., 2010). The finding that the velocity of motile *ron2* knockdown sporozoites in Matrigel is like that of control (Figure S10b) also supports that the major defect by *ron2* knockdown is the reduction in sporozoite attachment to the substrate, which might include basal lamina of mosquito salivary glands.

The mechanisms of sporozoite motility have been investigated by identification of related sporozoite proteins using the in vitro gliding assay (reviewed in Frischknecht & Matuschewski, 2017). Following activation with albumin treatment, incremental calcium release and a signal cascade in the parasite cytoplasm triggers secretion of adhesins, such as TRAP, from apical organelles to the surface to establish attachment to the substrate. Additionally, actin polymerisation strengthens

sporozoite attachment ability. The myosin motor then pushes actin filaments connected to several transmembrane adhesins towards the sporozoite posterior, which generates a force to move the parasite forward. From our study, RON2 is required for attachment to the substrate, which is an essential step for gliding, by acting as an adhesin, by mediating release of some adhesins, or by modifying actin polymerisation. It is possible that RON2 is released from rhoptries upon activation, as RON2 in merozoites is released prior to the invasion of erythrocytes. We failed to detect RON2 deposited in the gliding trail, possibly because the amount is lower than detectable or because it is not aggregated with CSP or TRAP. Detailed localization analysis of RON2 during gliding is required to address this question. Here, we demonstrated that the amount of TRAP was not decreased by ron2 knockdown (Figure S7a), unlike the observation following gene disruption of another gliding related protein, protein O-fucosylation 2 (POFUT2, Lopaticki et al., 2017). To investigate whether RON2 impacts the proper release of adhesins or dynamics of gliding related proteins, the expression and localization of known adhesins such as TREP/S6/UOS3, SIAP-1, and LIMP should be examined in ron2 knockdown sporozoites—and additionally with analysis of the behaviour of gliding related proteins such as ICP, CP, and plasmepsin VIII. Likewise, functional analysis of other RON complex members, that is, RON4 and RON5, during invasion of salivary glands would reveal whether they function co-ordinately in sporozoites as in merozoites.

3.4 | Contribution of RON2 to sporozoite transmission to mammalian hosts

We also sought to determine whether RON2 is also involved in migration to and/or invasion of hepatocytes. Ron2 knockdown decreased the abilities of cell traversal and invasion of hepatocytes and resulted in a reduction in the number of parasites in the liver after intravenous sporozoite inoculation. This phenotype reconciles previous studies demonstrating that mutant sporozoites with less attachment/gliding ability—such as TRAP-like protein (TLP) knockout, POFUT2 knockout, and S4/Celtos knockdown—show decreased cell traversal and/or cell invasion capacity (Lacroix & Ménard, 2008; Lopaticki et al., 2017; Steel et al., 2018). Therefore, it is indicated that decreased infectivity of ron2 knockdown sporozoites to mice is due to the defect in attachment/gliding ability. Notably, the effect of ron2 knockdown in cell traversal and invasion efficiency was not as crucial as in the invasion of salivary glands. There are possible explanations for this, including that Plasmodium sporozoites may have developed redundancies in their invasion machinery or that a minimal amount of RON2 (less than the detectable level by Western blot) is able to confer sufficient attachment of sporozoites to hepatocytes.

The processes underlying sporozoite invasion of hepatocytes and merozoite invasion of erythrocytes share several aspects, such as tight junction formation (Aikawa et al., 1978; Amino et al., 2008) and the subsequent proliferation inside the parasitophorous vacuole membrane. It has been demonstrated that the RON2 and AMA1 interaction has an essential role for tight junction formation during parasite invasion. Many investigations have pointed to a model whereby the AMA1-RONs complex acts as a parasite-derived receptor that enables

the parasite to invade several types of host cells (Besteiro et al., 2009; Besteiro, Dubremetz, & Lebrun, 2011). Recently, it was reported that the R1 peptide, an inhibitor of interaction between RON2 and AMA1, also diminished sporozoite cell traversal and invasion abilities in Pf to the same level as ron2 knockdown sporozoites demonstrated here (Yang et al., 2017). These results suggest that interaction between RON2 and AMA1 also has a key role, possibly via attachment ability, during sporozoite invasion. In contrast, however, results were reported that AMA1 is dispensable for invasion of salivary glands and hepatocytes in P. berghei (Bargieri et al., 2013; Giovannini et al., 2011). The discrepancy might be caused by the Plasmodium strain difference or the target specificity of the R1 peptide in sporozoites, and further analyses will be required to conclude whether the invasion mechanism is conserved between sporozoites and merozoites. If the counterpart of RON2 differs between stages, MAEBL could be a possible stage-specific counterpart in sporozoites, because it contains a region with high similarity to a region of AMA1 that contributes to the interaction with RON2 (Kappe, Noe, Fraser, Blair, & Adams, 1998; Vulliez-Le Normand et al., 2012) and maebl-disrupted sporozoites exhibited a phenotype similar to P_{msp1}- and P_{msp9}-RON2 sporozoites (Kariu et al., 2002; Saenz et al., 2008). These studies may shed light on which part is conserved or different among parasite species or infective stages in the molecular mechanisms of invasion.

Our sporozoite stage-specific knockdown system, in which the native promoter is replaced with the msp9 promoter, will help to elucidate the comprehensive mechanisms of rhoptry proteins in sporozoites. We demonstrate that RON2, one of the key molecules for merozoite invasion, is also involved in salivary gland and hepatocyte invasion, which confirms that merozoites and sporozoites have some common mechanisms to invade their target cells. On the other hand, the essentiality of RON2 differs between these invasion processes and suggests that parasite stage and target cell-specific mechanisms are likely involved. Elucidating the functions of other rhoptry proteins and identification of their counterpart proteins in sporozoites might reveal how Plasmodium parasites have developed efficient invasion mechanisms to adapt to specific host cells.

4 | EXPERIMENTAL PROCEDURES

4.1 | Parasites and mosquitoes

A transgenic P. berghei ANKA parasite line was used in this study, which constitutively expresses GFP under the control of the elongation factor 1A (ef1α) promoter without any drug resistance gene (Franke-Fayard et al., 2004). Cryopreserved P. berghei-infected erythrocytes were injected into female ICR mice (CLEA Japan, Tokyo, Japan) to obtain asexual and sexual stage parasites. For feeding experiments, infected ICR mice were fed to An. stephensi (SDA 500 strain) mosquitoes, and fully engorged mosquitoes were selected and kept at 20°C until dissection. At days 10–14 post feeding, the numbers of oocysts were examined to determine the prevalence. Sporozoites were collected from midguts or salivary glands by dissection at the indicated day post blood meal. Midgut sporozoites were purified by density gradient centrifugation using 17% Accudenz solution (Accurate Chemical

& Scientific Corporation, NY, United States; Kennedy et al., 2012). Haemolymph sporozoites were collected by infusion of RPMI 1640 medium (Wako Pure Chemical, Osaka, Japan) through the mosquito thorax (Kariu et al., 2002). Schizont-infected RBCs were purified using Nycoprep 1.077 solution (Axis-Shield Diagnostics, Dundee, UK) by centrifugation at 450×g for 20 min after 16 hr of culture of parasite infected RBCs in complete RPMI 1640 medium containing 20% fetal calf serum (FCS) with a gas mixture of 5% CO_2, 5% O_2, and 90% N_2 (Janse, Ramesar, & Waters, 2006). All animal experimental protocols were approved by the Institutional Animal Care and Use Committee of Ehime University, and the experiments were conducted according to the Ethical Guidelines for Animal Experiments of Ehime University.

4.2 | Preparation of antibodies against RON2 and HSP70

A recombinant *Pb*RON2 N-terminus protein, corresponding to the homologous region as a *Pf*RON2 antigen (Cao et al., 2009), was produced using the wheat germ cell-free translation system as described (Tsuboi et al., 2008). Briefly, DNA encoding the N-terminal region excluding the signal peptide, which corresponds to amino acids 22–91 of *Pb*RON2 (PBANKA_1315700), was amplified from *P. berghei* ANKA genomic DNA using Phusion high-fidelity DNA polymerase (New England BioLabs, Ipswich, MA, USA). The PCR product was then cloned into the pEU-E01-GST-TEV-N2 vector (CellFree Sciences, Matsuyama, Japan). *Pb*RON2-N GST fusion recombinant protein was expressed using the wheat germ cell-free protein synthesis system and then purified using a glutathione-sepharose column (GE Healthcare UK, Buckinghamshire, UK). The recombinant C-terminus of *Pb*HSP70 (PBANKA_0711900; amino acids 496–693) was produced using the method described above. Rabbits (Japanese white) were immunised subcutaneously with 250 μg of purified protein with Freund's adjuvant three times, and antisera was obtained 14 days after the final immunisation with recombinant protein (Kitayama labes, Ina, Japan).

4.3 | Western blotting

Protein homogenates of sporozoites collected at days 22–25 post feeding or enriched schizonts were dissolved in SDS-PAGE loading buffer with 10% ß-mercaptoethanol. The indicated number of parasites were subjected to electrophoresis on 7.5% polyacrylamide gels and then transferred to PVDF membranes using the wet-transfer system. Subsequent to blocking with Blocking One, the membrane was incubated with primary antibodies (1:2,500 for PbRON2-N and 1:250,000 for PbHSP70) for 1 hr at room temperature, followed by incubation with a secondary antibody conjugated to horseradish peroxidase (HRP; 1:30,000) for 30 min at room temperature. Chemiluminescence detection was performed by adding Immobilon Western Chemiluminescent HRP substrate (Merck Millipore, Darmstadt, Germany), then detecting the signal using ImageQuant LAS 4000 (GE Healthcare UK). Band intensities were measured using ImageQuant TL (GE Healthcare UK).

4.4 | Real-time RT-PCR

Total RNA was extracted from midguts, haemolymph, and salivary glands of mosquitoes infected with GFP or transgenic parasites on days 17 to 21 post feeding. Schizont-enriched infected RBCs were harvested for total RNA extraction (RNeasy, Qiagen GmbH, Hilden, Germany). Reverse transcription was conducted using the PrimeScript RT reagent Kit (Takara Bio, Otsu, Japan) with gDNA Eraser. Real-time RT-PCR reactions were performed using SYBR Premix Ex Taq (Takara Bio) according to the manufacturer's instructions. The primer sequences used are listed in Supporting Information. Real-time PCR was performed using the TaKaRa PCR Thermal Cycler Dice (Takara Bio). Relative gene expressions normalised by *ef1α* (PBANKA_1133300) or *rama* (PBANKA_0804500) mRNA level were compared using the delta-delta Ct method (Pfaffl, 2001).

4.5 | Immunotransmission electron microscopy

In vitro cultured schizonts, parasite-infected mosquito midguts, and salivary glands were fixed with 1% paraformaldehyde and 0.2% glutaraldehyde in 0.1 M Hepes buffer and then dehydrated and embedded in LR white resin. Ultrathin sections were blocked for 30 min in 0.1 M PBS containing 5% nonfat dry milk and 0.01% Tween 20 (PBS milk-Tween), followed by overnight incubation with specific rabbit antibodies in PBS milk-Tween. After washing with PBS containing 10% Block Ace and 0.01% Tween 20, samples were incubated for 1 hr in PBS milk-Tween containing goat anti-rabbit IgG conjugated to 15 nm of gold particles. The grids were then rinsed with distilled water, dried, and stained with 2% uranyl acetate in 50% methanol and lead citrate. Samples were examined with a transmission electron microscope (JEM-1230; JEOL, Tokyo, Japan).

4.6 | Generation of transgenic parasites

To generate RON2-c-Myc expressing transgenic parasites, the native *ron2* coding region in GFP parasites was replaced by single cross-over homologous recombination with an expression cassette of RON2 fused with a c-Myc tag at the C-terminus (see Figure S1). A *Toxoplasma* dihydrofolate reductase (DHFR) expressing cassette (*Tg*DHFR) was also integrated to confer pyrimethamine drug resistance in transgenic parasites. The transgenic DNA vector was a modification of the pL0033 plasmid, obtained from BEI Resource. The RON2 partial coding region (5,009–6,244 nt from the first methionine) was amplified using *Pb* genome DNA as a template and specific primers (Table S1), then cloned into pL0033 vector using SacII and NcoI restriction sites.

To generate sporozoite stage-specific *ron2* silencing transgenic parasites, the 5′UTR region of *ron2* was replaced with a merozoite-specific candidate promoter region by double cross-over homologous recombination within the GFP background strain (see Figure 3a). Two homologous recombination cassettes, *ron2* upstream (−1,683 to −845 bp relative to RON2 start of translation) and RON2-N (−105 to +945 bp) respectively, were subcloned into a transgenic vector containing a human DHFR expression cassette (hDHFR) used for drug selection (Otsuki et al., 2009). The promoter regions of *rap1* (−1,065 to −1 bp;

PBANKA_103210), *msp1* (−1,051 to −1 bp; PBANKA_083100), or *msp9* (−1,253 to −3 bp; PBANKA_144330) were also subcloned into the transgenic vector immediately before the RON2-N region. The constructed vectors used for transfection are shown in Figure S2.

Transfection of constructed DNA fragments into GFP parasites was performed as described (Janse et al., 2006). Briefly, 10 μg of MscI- or XhoI-linearized transfection vector was transfected into schizont-enriched GFP parasites by electroporation using Nucleofector (Lonza Japan, Tokyo, Japan). Transfected parasites were selected by adding 70 μg/ml of pyrimethamine to the drinking water after the parasites were inoculated into 4-week-old ICR female mice. Gene-modified parasites were cloned by limiting dilution, and DNA integration was confirmed by PCR genotyping. To confirm the phenotype of promoter swapping, two independent clones for P$_{msp9}$-RON2 were isolated from independent transfections and named P$_{msp9}$-RON2 cl1 and cl2. The primer sequences used are listed in Table S1.

4.7 | Indirect immunofluorescence analysis

Sporozoites were collected from parasite-infected mosquito midguts as described above, placed on glass slides, and then fixed by cold acetone for 2 min. Slides were blocked with Blocking ONE histo (nacalai tesque, Kyoto, Japan) for 30 min at 37°C, incubated with the anti-PbRON2-N antibodies (5.6 μg/ml) and anti CSP monoclonal antibody (1: 12,500, MRA-100; BEI Resources, Manassas, VA, USA) for 1 hr at 37°C, then incubated with Alexa Fluor 488-goat anti-rabbit IgG antibody and Alexa Fluor 546-goat anti-mouse IgG antibody (1:500) and 1 μg/ml 4′,6-diamidino-2-phenylindole (DAPI, Wako Pure Chemical). After mounting with ProLong Gold antifade reagent (Thermo Fisher Scientific), samples were observed with an inverted microscope (Axio Observer Z1, Carl Zeiss, Oberkochen, Germany), and data were acquired with an AxioCam MRm Charge-Coupled Device camera and AxioVision software (Carl Zeiss).

4.8 | Confocal microscopy observation of infected salivary glands

Salivary glands were collected by dissection of GFP or transgenic parasite-infected mosquitoes at days 24–26 post feeding, and then incubated with FM4-64 FX (5 μg/ml; Thermo Fisher Scientific) for salivary gland cellular membrane staining and DAPI (1 μg/ml; Wako Pure Chemical) in PBS for 20 min in a glass bottom culture dish. Salivary glands were observed with an LSM710 confocal microscope (Carl Zeiss). Images were assembled by ImageJ software (Schneider, Rasband, & Eliceiri, 2012) to show an approximately 5 μm stacked image (12 sections).

4.9 | Sporozoite gliding assay

At days 17–22 post feeding, sporozoites were collected from haemolymph by RPMI 1640 medium infusion through the mosquito thorax. For gliding assay on glass slides, sporozoites were mixed with the same volume of RPMI 1640 medium containing 20% FCS and placed in a glass bottom dish. For gliding assays in Matrigel, sporozoites in RPMI 1640 containing 20% FCS were mixed with an equal volume of Matrigel

(Corning, Corning, NY, USA), placed on glass slides, and covered with coverslips. Sporozoite movement was detected by GFP fluorescence using an AxioVert inverted fluorescence microscope (Carl Zeiss) and recorded with an AxioCam MRm Charge-Coupled Device camera (Carl Zeiss) every 2 s for up to 150 frames (5 min). Sporozoites on glass slides were classified manually as gliding, waving, or drifting according to Hegge et al. (2009). Experiments were repeated four times and at least 75 sporozoites were analysed for each parasite line. The effect of RON2 repression on sporozoite motility was evaluated by comparing the population of gliding sporozoite between P$_{rap1}$-RON2 and P$_{msp9}$-RON2 cl1 or cl2 by statistical analysis using the Mann–Whitney U test. In Matrigel, sporozoites were categorised as non-motile, circular movement, or meandering according to Volkmann et al (2012). The velocity of gliding sporozoites was calculated using MTrack2 plugin in Fiji software (NIH, Bethesda, MD).

4.10 | Sporozoite transmission assay by mosquito bite

For each parasite line, 20 infected mosquitoes (>65% prevalence) were placed in a new cage on days 21 to 22 post feeding and allowed to feed on a female C57BL/6 mouse (CREA Japan) for about 1 hr at rt. At 42 hr after feeding, the livers were perfused with PBS and removed to homogenise in 5 ml of Trizol (Thermo Fisher Scientific) using a polytron homogeniser (Kinematica AG, Luzern, Switzerland) for total RNA extraction. Reverse transcription and real-time PCR assays were performed as described above. The levels of parasite 18S rRNA were normalised to mouse *gapdh* mRNA expression. Expression levels of 18S rRNA were calculated by the ddCt method, and fold changes were obtained using the formula 2^{-ddCt} (Bruna-Romero et al., 2001). Experiments were performed using five to seven mice per mosquito group, and individual relative 18S rRNA levels, normalised by mouse *gapdh* mRNA amount, were plotted on the graph. Bars indicate the mean values for each parasite line. The difference in the relative 18S rRNA level among parasite lines was analysed by the Kruskal–Wallis test with a Dunn's post hoc test.

4.11 | In vivo liver infectivity

Equal number of sporozoites (5 or 10 thousand), collected from salivary glands of P$_{rap1}$-RON2 or P$_{msp9}$-RON2 cl1 infected mosquitoes at days 21–24 post feeding, were injected intravenously into female C57BL/6 mice (CLEA Japan). Twenty-four hours post inoculation, the livers were perfused and homogenised in 5 ml of Trizol (Thermo Fisher Scientific) for total RNA extraction, followed by real-time RT-PCR analysis as described above. This experiment was repeated twice, totally with six mice for each parasite line. The difference in the relative 18S rRNA level between P$_{rap1}$-RON2 and P$_{msp9}$-RON2 was analysed by the Mann–Whitney U test. The primers used in these experiments are listed in Table S1.

4.12 | In vitro sporozoite invasion analyses

The LS development assay was performed as described (Itani et al., 2014). Briefly, 3 to 10 thousand of P$_{rap1}$-RON2 or P$_{msp9}$-RON2

sporozoites collected from salivary glands were inoculated into HepG2 cells, a human hepatoma cell line, then incubated in RPMI 1640 media containing 10% FCS, 100 IU/ml penicillin, and 100 μg/ml streptomycin (Wako Pure Chemical) at 37°C in the presence of 5% CO_2 for 48 hr prior to fixation. Samples were stained with anti-CSP monoclonal antibodies (MRA-100) and anti-LISP2 antibodies to count the number of LS parasites and categorise the maturation stage per well (Itani et al., 2014). Experiments were repeated seven times with at least three wells for each line. The relative P_{msp9}-RON2 LS numbers normalised by control LS numbers were calculated. The proportions of LS maturation levels examined by LISP2 localization were examined. The effect of RON2 repression on LS number was evaluated by statistical analysis using the Mann–Whitney U test.

4.13 | In vitro sporozoite cell traversal assay

Cell traversal ability was assayed by the number of wounded cells 1 hr after sporozoite inoculation as described (Ishino et al., 2004). Briefly, 10,000 haemocoel sporozoites were incubated for 1 hr on confluent 3T3-Swiss albino cells in an eight-well chamber slide, with 1 mg/mL fluorescein conjugated dextran (MW 10,000, lysine fixable, Thermo Fisher Scientific) in RPMI 1640 medium containing 10% FCS. Cells were washed with PBS and fixed with 10% formalin. Fluorescence-labelled cells were counted under a fluorescence microscope (Axio Observer Z1, Carl Zeiss).

CONFLICT OF INTEREST

The authors have no conflict of interest.

ORCID

Tomoko Ishino http://orcid.org/0000-0003-2466-711X

REFERENCES

Aikawa, M., Miller, L. H., Johnson, J., & Rabbege, J. (1978). Erythrocyte entry by malarial parasites. A moving junction between erythrocyte and parasite. *The Journal of Cell Biology*, 77(1), 72–82. https://doi.org/10.1083/jcb.77.1.72

Amino, R., Giovannini, D., Thiberge, S., Gueirard, P., Boisson, B., Dubremetz, J. F., ... Menard, R. (2008). Host cell traversal is important for progression of the malaria parasite through the dermis to the liver. *Cell Host & Microbe*, 3(2), 88–96. doi: S1931-3128(08)00002-4 [pii]. https://doi.org/10.1016/j.chom.2007.12.007

Arumugam, T. U., Ito, D., Takashima, E., Tachibana, M., Ishino, T., Torii, M., & Tsuboi, T. (2014). Application of wheat germ cell-free protein expression system for novel malaria vaccine candidate discovery. *Expert Review of Vaccines*, 13(1), 75–85. https://doi.org/10.1586/14760584.2014.861747

Aurrecoechea, C., Brestelli, J., Brunk, B. P., Dommer, J., Fischer, S., Gajria, B., ... Wang, H. (2009). PlasmoDB: A functional genomic database for malaria parasites. *Nucleic Acids Research*, 37(Database issue), D539–D543. doi:gkn814 [pii]. https://doi.org/10.1093/nar/gkn814

Bargieri, D. Y., Andenmatten, N., Lagal, V., Thiberge, S., Whitelaw, J. A., Tardieux, I., ... Menard, R. (2013). Apical membrane antigen 1 mediates apicomplexan parasite attachment but is dispensable for host cell invasion. *Nature Communications*, 4, 2552. doi:ncomms3552 [pii]. https://doi.org/10.1038/ncomms3552

Beck, J. R., Fung, C., Straub, K. W., Coppens, I., Vashisht, A. A., Wohlschlegel, J. A., & Bradley, P. J. (2013). A *Toxoplasma* palmitoyl acyl transferase and the palmitoylated armadillo repeat protein TgARO govern apical rhoptry tethering and reveal a critical role for the rhoptries in host cell invasion but not egress. *PLoS Pathogens*, 9(2), e1003162. https://doi.org/10.1371/journal.ppat.1003162. PPATHOGENS-D-12-02397 [pii]

Besteiro, S., Dubremetz, J. F., & Lebrun, M. (2011). The moving junction of apicomplexan parasites: A key structure for invasion. *Cellular Microbiology*, 13(6), 797–805. https://doi.org/10.1111/j.1462-5822.2011.01597.x

Besteiro, S., Michelin, A., Poncet, J., Dubremetz, J. F., & Lebrun, M. (2009). Export of a *Toxoplasma gondii* rhoptry neck protein complex at the host cell membrane to form the moving junction during invasion. *PLoS Pathogens*, 5(2), e1000309. https://doi.org/10.1371/journal.ppat.1000309

Boysen, K. E., & Matuschewski, K. (2013). Inhibitor of cysteine proteases is critical for motility and infectivity of *Plasmodium sporozoites*. *MBio*, 4(6), e00874–e00813. doi:mBio.00874-13 [pii]. https://doi.org/10.1128/mBio.00874-13

Bruna-Romero, O., Hafalla, J. C., Gonzalez-Aseguinolaza, G., Sano, G., Tsuji, M., & Zavala, F. (2001). Detection of malaria liver-stages in mice infected through the bite of a single Anopheles mosquito using a highly sensitive real-time PCR. *International Journal for Parasitology*, 31(13), 1499–1502. https://doi.org/10.1016/S0020-7519(01)00265-X

Campbell, T. L., De Silva, E. K., Olszewski, K. L., Elemento, O., & Llinas, M. (2010). Identification and genome-wide prediction of DNA binding specificities for the ApiAP2 family of regulators from the malaria parasite. *PLoS Pathogens*, 6(10), e1001165. https://doi.org/10.1371/journal.ppat.1001165

Cao, J., Kaneko, O., Thongkukiatkul, A., Tachibana, M., Otsuki, H., Gao, Q., ... Torii, M. (2009). Rhoptry neck protein RON2 forms a complex with microneme protein AMA1 in *Plasmodium falciparum* merozoites. *Parasitology International*, 58(1), 29–35. doi: S1383-5769(08)00111-6 [pii]. https://doi.org/10.1016/j.parint.2008.09.005

Combe, A., Giovannini, D., Carvalho, T. G., Spath, S., Boisson, B., Loussert, C., ... Menard, R. (2009). Clonal conditional mutagenesis in malaria parasites. *Cell Host & Microbe*, 5(4), 386–396. doi: S1931-3128(09)00099-7 [pii]. https://doi.org/10.1016/j.chom.2009.03.008

Combe, A., Moreira, C., Ackerman, S., Thiberge, S., Templeton, T. J., & Menard, R. (2009). TREP, a novel protein necessary for gliding motility of the malaria sporozoite. *International Journal for Parasitology*, 39(4), 489–496. doi: S0020-7519(08)00382-2 [pii]. https://doi.org/10.1016/j.ijpara.2008.10.004

De Silva, E. K., Gehrke, A. R., Olszewski, K., Leon, I., Chahal, J. S., Bulyk, M. L., & Llinas, M. (2008). Specific DNA-binding by apicomplexan AP2 transcription factors. *Proceedings of the National Academy of Sciences of the United States of America*, 105(24), 8393–8398. doi:0801993105 [pii]. https://doi.org/10.1073/pnas.0801993105

Douglas, R. G., Amino, R., Sinnis, P., & Frischknecht, F. (2015). Active migration and passive transport of malaria parasites. *Trends in Parasitology*, 31(8), 357–362. https://doi.org/10.1016/j.pt.2015.04.010

Dvorin, J. D., Martyn, D. C., Patel, S. D., Grimley, J. S., Collins, C. R., Hopp, C. S., ... Duraisingh, M. T. (2010). A plant-like kinase in *Plasmodium*

falciparum regulates parasite egress from erythrocytes. *Science*, *328*(5980), 910–912. doi:328/5980/910 [pii]. https://doi.org/10.1126/science.1188191

Ejigiri, I., Ragheb, D. R., Pino, P., Coppi, A., Bennett, B. L., Soldati-Favre, D., & Sinnis, P. (2012). Shedding of TRAP by a rhomboid protease from the malaria sporozoite surface is essential for gliding motility and sporozoite infectivity. *PLoS Pathogens*, *8*(7), e1002725. https://doi.org/10.1371/journal.ppat.1002725. PPATHOGENS-D-11-01012 [pii]

Engelmann, S., Silvie, O., & Matuschewski, K. (2009). Disruption of *Plasmodium* sporozoite transmission by depletion of sporozoite invasion-associated protein 1. *Eukaryotic Cell*, *8*(4), 640–648. https://doi.org/10.1128/EC.00347-08

Franke-Fayard, B., Trueman, H., Ramesar, J., Mendoza, J., van der Keur, M., van der Linden, R., ... Janse, C. J. (2004). A *Plasmodium berghei* reference line that constitutively expresses GFP at a high level throughout the complete life cycle. *Molecular and Biochemical Parasitology*, *137*(1), 23–33. https://doi.org/10.1016/j.molbiopara.2004.04.007. S0166685 104001173 [pii]

Frischknecht, F., & Matuschewski, K. (2017). *Plasmodium* sporozoite biology. Malaria: Biology in the era of eradication. *Cold Spring Harbor Perspectives in Medicine*, *7*(5), 99–112. https://doi.org/10.1101/cshperspect.a025478.

Ganter, M., Schüler, H., & Matuschewski, K. (2009). Vital role for the *Plasmodium* actin capping protein (CP) beta-subunit in motility of malaria sporozoites. *Molecular Microbiology*, *74*(6), 1356–1367. https://doi.org/10.1111/j.1365-2958.2009.06828.x

Ghosh, A. K., & Jacobs-Lorena, M. (2009). *Plasmodium* sporozoite invasion of the mosquito salivary gland. *Current Opinion in Microbiology*, *12*(4), 394–400. doi: S1369-5274(09)00079-4 [pii]. https://doi.org/10.1016/j.mib.2009.06.010

Giovannini, D., Spath, S., Lacroix, C., Perazzi, A., Bargieri, D., Lagal, V., ... Menard, R. (2011). Independent roles of apical membrane antigen 1 and rhoptry neck proteins during host cell invasion by apicomplexa. *Cell Host & Microbe*, *10*(6), 591–602. doi: S1931-3128(11)00365-9 [pii]. https://doi.org/10.1016/j.chom.2011.10.012

Hegge, S., Kudryashev, M., Smith, A., & Frischknecht, F. (2009). Automated classification of *Plasmodium* sporozoite movement patterns reveals a shift towards productive motility during salivary gland infection. *Biotechnology Journal*, *4*(6), 903–913. https://doi.org/10.1002/biot.200900007

Hegge, S., Münter, S., Steinbüchel, M., Heiss, K., Engel, U., Matuschewski, K., & Frischknecht, F. (2010). Multistep adhesion of Plasmodium sporozoites. *FASEB J.*, *24*(7): 2222–2234. https://doi.org/10.1096/fj.09-148700

Ishino, T., Yano, K., Chinzei, Y., & Yuda, M. (2004). Cell-passage activity is required for the malarial parasite to cross the liver sinusoidal cell layer. *PLoS Biology*, *2*(1), E4. https://doi.org/10.1371/journal.pbio.0020004

Itani, S., Torii, M., & Ishino, T. (2014). D-Glucose concentration is the key factor facilitating liver stage maturation of *Plasmodium*. *Parasitology International*, *63*(4), 584–590. https://doi.org/10.1016/j.parint.2014.03.004

Janse, C. J., Ramesar, J., & Waters, A. P. (2006). High-efficiency transfection and drug selection of genetically transformed blood stages of the rodent malaria parasite *Plasmodium berghei*. *Nature Protocols*, *1*(1), 346–356. doi:nprot.2006.53 [pii]. https://doi.org/10.1038/nprot.2006.53

Kappe, S. H., Noe, A. R., Fraser, T. S., Blair, P. L., & Adams, J. H. (1998). A family of chimeric erythrocyte binding proteins of malaria parasites. *Proceedings of the National Academy of Sciences of the United States of America*, *95*(3), 1230–1235. https://doi.org/10.1073/pnas.95.3.1230

Kariu, T., Yuda, M., Yano, K., & Chinzei, Y. (2002). MAEBL is essential for malarial sporozoite infection of the mosquito salivary gland. *The Journal of Experimental Medicine*, *195*(10), 1317–1323. https://doi.org/10.1084/jem.20011876

Kennedy, M., Fishbaugher, M. E., Vaughan, A. M., Patrapuvich, R., Boonhok, R., Yimamnuaychok, N., ... Lindner, S. E. (2012). A rapid and scalable density gradient purification method for *Plasmodium sporozoites*. *Malaria Journal*, 11, 421. https://doi.org/10.1186/1475-2875-11-421

Lacroix, C., & Ménard, R. (2008). TRAP-like protein of *Plasmodium sporozoites*: linking gliding motility to host-cell traversal. *Trends in Parasitology*, *24*(10), 431–434. https://doi.org/10.1016/j.pt.2008.07.003

Lamarque, M., Besteiro, S., Papoin, J., Roques, M., Vulliez-Le Normand, B., Morlon-Guyot, J., ... Lebrun, M. (2011). The RON2-AMA1 interaction is a critical step in moving junction-dependent invasion by apicomplexan parasites. *PLoS Pathogens*, *7*(2), e1001276. https://doi.org/10.1371/journal.ppat.1001276

Lebrun, M., Michelin, A., El Hajj, H., Poncet, J., Bradley, P. J., Vial, H., & Dubremetz, J. F. (2005). The rhoptry neck protein RON4 re-localizes at the moving junction during *Toxoplasma gondii* invasion. *Cellular Microbiology*, *7*(12), 1823–1833. https://doi.org/10.1111/j.1462-5822.2005.00646.x

Lindner, S. E., Swearingen, K. E., Harupa, A., Vaughan, A. M., Sinnis, P., Moritz, R. L., & Kappe, S. H. (2013). Total and putative surface proteomics of malaria parasite salivary gland sporozoites. *Molecular & Cellular Proteomics*, *12*(5), 1127–1143. doi: M112.024505 [pii]. https://doi.org/10.1074/mcp. M112.024505

Lopaticki, S., Yang, A. S. P., John, A., Scott, N. E., Lingford, J. P., O'Neill, M. T., ... Boddey, J. A. (2017). Protein O-fucosylation in *Plasmodium falciparum* ensures efficient infection of mosquito and vertebrate hosts. *Nature Communications*, *8*(1), 561. https://doi.org/10.1038/s41467-017-00571-y.

Mastan, B. S., Narwal, S. K., Dey, S., Kumar, K. A., & Mishra, S. (2017). *Plasmodium berghei* plasmepsin VIII is essential for sporozoite gliding motility. *International Journal for Parasitology*, *47*(5), 239–245. https://doi.org/10.1016/j.ijpara.2016.11.009

Mikolajczak, S. A., Silva-Rivera, H., Peng, X., Tarun, A. S., Camargo, N., Jacobs-Lorena, V., ... Kappe, S. H. (2008). Distinct malaria parasite sporozoites reveal transcriptional changes that cause differential tissue infection competence in the mosquito vector and mammalian host. *Molecular and Cellular Biology*, *28*(20), 6196–6207. https://doi.org/10.1128/MCB.00553-08

Modrzynska, K., Pfander, C., Chappell, L., Yu, L., Suarez, C., Dundas, K., ... Billker, O. (2017). A knockout screen of ApiAP2 genes reveals networks of interacting transcriptional regulators controlling the *Plasmodium* life cycle. *Cell Host & Microbe*, *21*(1), 11–22. doi: S1931-3128(16)30514-5 [pii]. https://doi.org/10.1016/j.chom.2016.12.003

Morahan, B. J., Wang, L., & Coppel, R. L. (2008). No TRAP, no invasion. *Trends in Parasitol*, *12*(5), 77–84. https://doi.org/10.1016/j.pt.2008.11.004

Mueller, A. K., Camargo, N., Kaiser, K., Andorfer, C., Frevert, U., Matuschewski, K., & Kappe, S. H. (2005). Plasmodium liver stage developmental arrest by depletion of a protein at the parasite-host interface. *Proceedings of the National Academy of Sciences of the United States of America*, *102*(8), 3022–3027. doi:0408442102 [pii]. https://doi.org/10.1073/pnas.0408442102

Mueller, A. K., Kohlhepp, F., Hammerschmidt, C., & Michel, K. (2010). Invasion of mosquito salivary glands by malaria parasites: Prerequisites and defense strategies. *International Journal for Parasitology*, *40*(11), 1229–1235. doi: S0020-7519(10)00186-4 [pii]. https://doi.org/10.1016/j.ijpara.2010.05.005

Münter, S., Sabass, B., Selhuber-Unkel, C., Kudryashev, M., Hegge, S., Engel, U., ... Frischknecht, F. (2009). *Plasmodium* sporozoite motility is modulated by the turnover of discrete adhesion sites. *Cell Host & Microbe*, *6*(6), 551–562. https://doi.org/10.1016/j.chom.2009.11.007

Mutungi, J. K., Yahata, K., Sakaguchi, M., & Kaneko, O. (2014). Expression and localization of rhoptry neck protein 5 in merozoites and sporozoites of *Plasmodium yoelii*. *Parasitology International*, *63*(6), 794–801. doi: S1383-5769(14)00104-4 [pii]. https://doi.org/10.1016/j.parint.2014.07.013

Otsuki, H., Kaneko, O., Thongkukiatkul, A., Tachibana, M., Iriko, H., Takeo, S., ... Torii, M. (2009). Single amino acid substitution in *Plasmodium yoelii* erythrocyte ligand determines its localization and controls parasite virulence. *Proceedings of the National Academy of Sciences of the United States of America*, *106*(17), 7167–7172. doi:0811313106 [pii]. https://doi.org/10.1073/pnas.0811313106

Pfaffl, M. W. (2001). A new mathematical model for relative quantification in real-time RT-PCR. *Nucleic Acids Research*, *29*(9), e45–e445. https://doi.org/10.1093/nar/29.9.e45

Pimenta, P. F., Touray, M., & Miller, L. (1994). The journey of malaria sporozoites in the mosquito salivary gland. *The Journal of Eukaryotic Microbiology*, *41*(6), 608–624. https://doi.org/10.1111/j.1550-7408.1994.tb01523.x

Poukchanski, A., Fritz, H. M., Tonkin, M. L., Treeck, M., Boulanger, M. J., & Boothroyd, J. C. (2013). *Toxoplasma gondii* sporozoites invade host cells using two novel paralogues of RON2 and AMA1. *PLoS One*, *8*(8), e70637. https://doi.org/10.1371/journal.pone.0070637. PONE-D-13-18538 [pii]

Richard, D., MacRaild, C. A., Riglar, D. T., Chan, J. A., Foley, M., Baum, J., ... Cowman, A. F. (2010). Interaction between *Plasmodium falciparum* apical membrane antigen 1 and the rhoptry neck protein complex defines a key step in the erythrocyte invasion process of malaria parasites. *The Journal of Biological Chemistry*, *285*(19), 14815–14822. doi: M109.080770 [pii]. https://doi.org/10.1074/jbc. M109.080770

Risco-Castillo, V., Topcu, S., Son, O., Briquet, S., Manzoni, G., & Silvie, O. (2014). CD81 is required for rhoptry discharge during host cell invasion by *Plasmodium yoelii* sporozoites. *Cellular Microbiology*, *16*(10), 1533–1548. https://doi.org/10.1111/cmi.12309

Saenz, F. E., Balu, B., Smith, J., Mendonca, S. R., & Adams, J. H. (2008). The transmembrane isoform of *Plasmodium falciparum* MAEBL is essential for the invasion of *Anopheles* salivary glands. *PLoS One*, *3*(5), e2287. https://doi.org/10.1371/journal.pone.0002287

Santos, J. M., Egarter, S., Zuzarte-Luís, V., Kumar, H., Moreau, C. A., Kehrer, J., ... Mair, G. R. (2017). Malaria parasite LIMP protein regulates sporozoite gliding motility and infectivity in mosquito and mammalian hosts. *eLife*, *6*, e24109. https://doi.org/10.7554/eLife.24109

Schneider, C. A., Rasband, W. S., & Eliceiri, K. W. (2012). NIH image to ImageJ: 25 years of image analysis. *Nature Methods*, *9*(7), 671–675. https://doi.org/10.1038/nmeth.2089

Siden-Kiamos, I., Ganter, M., Kunze, A., Hliscs, M., Steinbuchel, M., Mendoza, J., ... Matuschewski, K. (2011). Stage-specific depletion of myosin A supports an essential role in motility of malarial ookinetes. *Cellular Microbiology*, *13*(12), 1996–2006. https://doi.org/10.1111/j.1462-5822.2011.01686.x

Smith, R. C., & Jacobs-Lorena, M. (2010). Plasmodium-mosquito interactions: A tale of roadblocks and detours. *Adv In Insect Phys*, *39*, 119–149. https://doi.org/10.1016/B978-0-12-381387-9.00004-X

Srinivasan, P., Beatty, W. L., Diouf, A., Herrera, R., Ambroggio, X., Moch, J. K., ... Miller, L. H. (2011). Binding of *Plasmodium* merozoite proteins RON2 and AMA1 triggers commitment to invasion. *Proceedings of the National Academy of Sciences of the United States of America*, *108*(32), 13275–13280. doi:1110303108 [pii]. https://doi.org/10.1073/pnas.1110303108

Steel, R. W. J., Pei, Y., Camargo, N., Kaushansky, A., Dankwa, D. A., Martinson, T., ... Kappe, S. H. I. (2018). *Plasmodium yoelii* S4/CelTOS is important for sporozoite gliding motility and cell traversal. *Cellular Microbiology*, *20*(4), e12817. https://doi.org/10.1111/cmi.12817

Steinbuechel, M., & Matuschewski, K. (2009). Role for the *Plasmodium* sporozoite-specific transmembrane protein S6 in parasite motility and efficient malaria transmission. *Cellular Microbiology*, *11*(2), 279–288. doi: CMI1252 [pii]. https://doi.org/10.1111/j.1462-5822.2008.01252.x

Sterling, C. R., Aikawa, M., & Vanderberg, J. P. (1973). The passage of *Plasmodium berghei* sporozoites through the salivary glands of *Anopheles stephensi*: An electron microscope study. *The Journal of Parasitology*, *59*(4), 593–605. https://doi.org/10.2307/3278847

Sultan, A. A., Thathy, V., Frevert, U., Robson, K. J., Crisanti, A., Nussenzweig, V., ... Menard, R. (1997). TRAP is necessary for gliding motility and infectivity of *Plasmodium sporozoites*. *Cell*, *90*(3), 511–522. doi: S0092-8674(00)80511-5 [pii], DOI: https://doi.org/10.1016/S0092-8674(00)80511-5

Tonkin, M. L., Roques, M., Lamarque, M. H., Pugniere, M., Douguet, D., Crawford, J., ... Boulanger, M. J. (2011). Host cell invasion by apicomplexan parasites: Insights from the co-structure of AMA1 with a RON2 peptide. *Science*, *333*(6041), 463–467. doi:333/6041/463 [pii]. https://doi.org/10.1126/science.1204988

Topolska, A. E., Black, C. G., & Coppel, R. L. (2004). Identification and characterisation of RAMA homologues in rodent, simian and human malaria species. *Molecular and Biochemical Parasitology*, *138*(2), 237–241. https://doi.org/10.1016/j.molbiopara.2004.05.018

Tsuboi, T., Takeo, S., Arumugam, T. U., Otsuki, H., & Torii, M. (2010). The wheat germ cell-free protein synthesis system: A key tool for novel malaria vaccine candidate discovery. *Acta Tropica*, *114*(3), 171–176. doi: S0001-706X(09)00360-X [pii]. https://doi.org/10.1016/j.actatropica.2009.10.024

Tsuboi, T., Takeo, S., Iriko, H., Jin, L., Tsuchimochi, M., Matsuda, S., ... Endo, Y. (2008). Wheat germ cell-free system-based production of malaria proteins for discovery of novel vaccine candidates. *Infection and Immunity*, *76*(4), 1702–1708. doi: IAI.01539-07 [pii]. https://doi.org/10.1128/IAI.01539-07

Tufet-Bayona, M., Janse, C. J., Khan, S. M., Waters, A. P., Sinden, R. E., & Franke-Fayard, B. (2009). Localisation and timing of expression of putative *Plasmodium berghei* rhoptry proteins in merozoites and sporozoites. *Molecular and Biochemical Parasitology*, *166*(1), 22–31. doi: S0166-6851(09)00067-X [pii]. https://doi.org/10.1016/j.molbiopara.2009.02.009

Tyler, J. S., & Boothroyd, J. C. (2011). The C-terminus of *Toxoplasma* RON2 provides the crucial link between AMA1 and the host-associated invasion complex. *PLoS Pathogens*, *7*(2), e1001282. https://doi.org/10.1371/journal.ppat.1001282

Volkmann, K., Pfander, C., Burstroem, C., Ahras, M., Goulding, D., Rayner, J. C., ... Brochet, M. (2012). The alveolin IMC1h is required for normal ookinete and sporozoite motility behaviour and host colonisation in *Plasmodium berhgei*. *PLoS One*, *7*(7), e41409. https://doi.org/10.1371/journal.pone.0041409

Vulliez-Le Normand, B., Tonkin, M. L., Lamarque, M. H., Langer, S., Hoos, S., Roques, M., ... Lebrun, M. (2012). Structural and functional insights into the malaria parasite moving junction complex. *PLoS Pathogens*, *8*(6), e1002755. https://doi.org/10.1371/journal.ppat.1002755. PPATHOGENS-D-11-02790 [pii]

WHO. (2017). World malaria report.

Yang, A. S. P., Lopaticki, S., O'Neill, M. T., Erickson, S. M., Douglas, D. N., Kneteman, N. M., & Boddey, J. A. (2017). AMA1 and MAEBL are important for *Plasmodium falciparum* sporozoite infection of the liver. *Cellular Microbiology*, *19*(9), e12745. https://doi.org/10.1111/cmi.12745

Yap, A., Azevedo, M. F., Gilson, P. R., Weiss, G. E., O'Neill, M. T., Wilson, D. W., ... Cowman, A. F. (2014). Conditional expression of apical membrane antigen 1 in *Plasmodium falciparum* shows it is required for erythrocyte invasion by merozoites. *Cellular Microbiology*, *16*(5), 642–656. https://doi.org/10.1111/cmi.12287

Young, J. A., Johnson, J. R., Benner, C., Yan, S. F., Chen, K., Le Roch, K. G., ... Winzeler, E. A. (2008). In silico discovery of transcription regulatory elements in *Plasmodium falciparum*. *BMC Genomics*, *9*, 70. doi:1471-2164-9-70 [pii]. https://doi.org/10.1186/1471-2164-9-70

SUPPORTING INFORMATION

Additional supporting information may be found online in the Supporting Information section at the end of the article.